JOURNAL OF CATALYSIS **147**, 223–230 (1994)

IR Study of Brønsted Acidity of Al-Pillared Montmorillonite

Silvia Bodoardo,*,† François Figueras,‡ and Edoardo Garrone*,[1]

**Dipartimento di Chimica Inorganica, Chimica Fisica e Chimica dei Materiali, Università di Torino, Via P. Giuria 7, 10125 Torino, Italy; †Dipartimento di Scienza dei Materiali ed Ingegneria Chimica Politecnico di Torino, Corso Duca degli Abruzzi 24, 10129 Torino, Italy; and ‡Laboratoire de Chimie Organique Physique e Cinétique Chimique Appliquées, UA 418 du CNRS, Ecole Nationale Supérieure de Chimie de Montpellier, 8 rue Ecole Normale, 34075 Montpellier Cedex, France*

Received February 12, 1993; revised November 24, 1993

Three different methods have been used to study the hydroxyls of montmorillonite, both as such and pillared with Al_{13} polycations. The methods are (i) formation of H-bonds with benzene, (ii) selective H/D exchange, and (iii) adsorption of pyridine. Besides non-acidic species, two reactive hydroxyls have been identified, characterized by stretching modes at 3738 and 3660 cm^{-1}. The former is ascribed to a species Al–O–Si–OH, resembling the hydroxyl on silica, and the latter to a species Si–O–Al–OH, similar to extraframework species in zeolites. Both arise from sealing the clay sheet and the Al pillar; their acidity comes from a synergic effect between the two constituents, as similar species in both silica and alumina are definitely less acidic. No bridged species Si(OH)Al is formed. Pyridine adsorption shows that (i) only the Si–O–Al–OH species may transfer protons, (ii) at least two distinct Lewis acid sites are present, and (iii) one of the related pyridine species reacts with a nearby hydroxyl to yield α-pyridone.

INTRODUCTION

Clays have long been used as acidic catalysts in petroleum cracking. Interest is currently focused on pillared clays (PILC), where large two-dimensional pores allow large molecules to react, although maintaining some shape selectivity (1).

Brønsted and Lewis acidity of such systems is classically studied by following, mainly in the IR, the adsorption of pyridine and ammonia. In pure montmorillonite, hydration water is the main source of Brønsted acidity (2–4); deuteration of lattice hydroxyls proceeds rapidly in the presence of D_2O, and Lewis acidity may be present. As to cross-linked beidellites, it has been shown that their acidity, after treatment at 770 K, is mainly of the Lewis type and related to the pillars (5), whereas Brønsted acidity (6) is due to the protonation of Si–O–Al bridges, originating, as in zeolites, from the substitution of silicon by aluminum atoms in the tetrahedral sheet; consequently, beidellite has a Brønsted acidity stronger than that of pillared montmorillonite, in which Si/Al substitution does not take place.

As to pillared montmorillonites, Tichit *et al.* (7) observed that Brønsted acidity is weak, as pyridinium ions disappear upon thermal treatments above 570 K, whereas Lewis sites are strong and hold pyridine up to 750 K; the acidity of PILCs as a whole is comparable to that of Zeolite Y. Shabtai *et al.* (8) found that Ce-exchanged, Al-pillared montmorillonite has a larger proportion of Lewis sites than of Brønsted sites. More detailed work has been carried out by Occelli *et al.* (9, 10) and Ming-Yuan *et al.* (11). Two types of hydroxyls have been found, absorbing, respectively, at 3740 and 3670 cm^{-1}, both with acidic character (9, 10); it was also concluded (11) that pillars provide sites for Lewis acidity, but not for Brønsted acidity. This latter has been ascribed (11) to the clay layers; it has been noticed, however, that by no means are the acidity and other properties of PILC the sum of those of the two constituents.

Although a good deal of data is available, a more detailed IR characterization of hydroxyls in PILCs is possible. In the present paper, a systematic study is given concerning Al-pillared montmorillonite, the original substance being used basically for comparison. Hydroxyls are studied by careful examination of the O–H stretching region by measuring their strength of H-bonding with a suitable molecule, the ease of H/D isotopic exchange, and the propensity toward proton transfer to pyridine. In order to make the system simpler, a large fraction of hydroxyls has been eliminated by adopting high pretreatment temperatures. Future papers on the same systems will deal with ammonia adsorption and reaction with hydrocarbons.

EXPERIMENTAL

Two samples were studied. One was an original Greek montmorillonite (clay G) whose structural formula is

$$(Si_{2.56}Al_{0.44})^{IV}(Al_{2.46}Fe_{0.69}Mg_{0.74}Ti_{0.08})^{VI}(Ca_{0.26}Na_{0.22}K_{0.28})O_{20}H_4,$$

---

[1] To whom correspondence should be addressed.

0021-9517/94 $6.00

where the symbols IV and VI indicate tetrahedral and octahedral coordination of the atoms, respectively.

The other sample was the same clay intercalated with aluminum hydroxy-polycation Al_{13} (clay A) (12). The pillaring process was carried out by adding 5 mmole of $Al(OH)_3$ per g of the starting clay. Pores are in the range 20–60 Å and BET areas in the range 140–240 m^2/g (13). Some ancillary data have also been collected concerning samples of clay A which underwent some H^+/Ce^{3+} exchange (clay Ce).

Thin pellets of the samples were pressed and placed into a quartz IR cell fitted with KBr windows. The cell is suitable for thermal treatment *in vacuo* (10^{-3} Pa) and for dosing gases *in situ*. Unless otherwise specified, pretreatment temperature was 770 K. IR measurements have been performed on a FTIR spectrophotometer (Perkin–Elmer 1720) connected to a data station (P–E 7500).

RESULTS

Spectra of the Bare Samples in the Hydroxyl Region

The spectra of samples G and A, together with that of clay Ce, after outgassing at 770 K, are reported in Fig. 1a. In all cases, a rather intense absorption is observed, so that the spectra are reported in transmission. Figure 2 reports a magnification of the range 3600–3800 cm^{-1} in order to show the small but significant changes that occurred. Clay G shows a peak at 3744 cm^{-1} due to the OH stretching of SiOH species similar to silanol groups, which absorb at 3747 cm^{-1} on silica or the external surfaces of zeolites (14). Such hydroxyls are either located at corners and fractures of sheets or are formed by the process of tetrahedra inversion (15), i.e., the rearrangement which may take place in the two outer Si–O layers (of the three constituting the clay sheet), by which the Si–O–Al bond is hydrolyzed, and the Si atom acquires a hydroxyl, pointing outwards. Such a process is thought to be important in the pillaring mechanism of the clay, and indeed the same band is present on clay A with a lower intensity, thereby showing that related species are involved in the pillaring process.

In clay A, a new band is found at 3738 cm^{-1} (Fig. 2), which is likely to be due to SiOH species perturbed by pillars; in the following, it is designated as (SiOH)*. In the exchange process leading to clay Ce, protons have been substituted to some extent by the Ce cations according to their acidity; indeed, the 3738 cm^{-1} species is no longer seen. A residue of the original 3744 cm^{-1} species is the only feature in the high-frequency region of the OH stretch, which indicates the less acidic nature of such OH species.

A weak shoulder at 3715 cm^{-1} is observed in all clays. Such a frequency is characteristic of isolated hydroxyl groups on octahedral aluminum (14) in Al_2O_3. A similar interpretation is proposed here, involving cations in the octahedral sheet and possibly in pillars in the case of clays A and Ce. Accordingly, the hydroxyl species is designated as $Al^{VI}OH$.

The most evident feature of the spectra is a broadband, centered at 3660 cm^{-1}, which can be related to various types of OH groups on aluminum ions and, if present, Si(OH)Al bridged species formed upon pillaring. Exchange with Ce ions depletes only the low-frequency component of the band envelope.

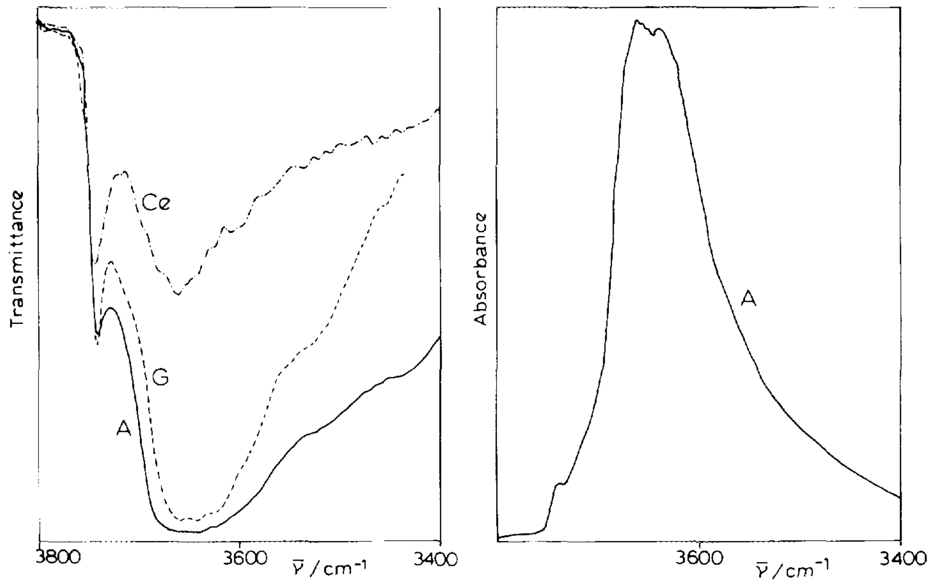

FIG. 1. IR spectra of the hydroxyl stretching region of clays G, A, and Ce outgassed at 770 K. Left side (transmittance vs wavenumber): conventional samples; (—) clay A; (---) clay G; (-·-) clay Ce. Right side (absorbance vs wavenumber): ultrathin pellet of clay A.

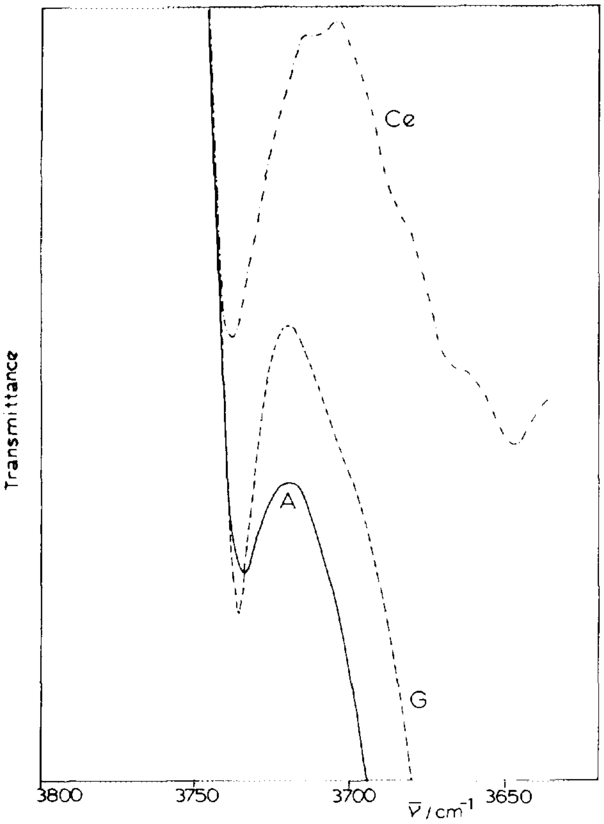

FIG. 2. Magnification of the 3600–3800 cm^{-1} region of Fig. 1, left side.

Other features in Fig. 1a below 3500 cm^{-1}, e.g., the component around 3400 cm^{-1}, are due to hydrogen-bonded species.

Figure 1b shows the spectrum of an exceptionally thin pellet of clay A. Because of the increase in transparency, the spectrum is shown here in absorbance, which allows the observation of two components at 3660 and 3640 cm^{-1} (besides that of the band at 3738 cm^{-1} and the shoulder at 3715 cm^{-1}); the corresponding species are indicated in the following as $(AlOH)_1$ and $(AlOH)_2$, respectively. Absorption is, however, weak around 3610 cm^{-1}, where bridged species are expected to fall.

For the sake of clarity, the spectral features of the various OH species are gathered in Table 1.

Hydrogen Bond Formation

For such a study, a weakly basic molecule is needed to avoid proton transfer. Following a suggestion by Kustov *et al.* (16), we have used benzene (actually d_6-benzene, as the same substance was also employed as the deuterating agent, as shown below).

TABLE 1

Stretching Frequencies (cm^{-1}) of the various Hydroxyl Species, as Such and after Mild Deuteration with C_6D_6, and Shifts Caused by Interaction with Benzene

System	ν(OH)	$\Delta\nu$(OH)	ν(OD)	$\Delta\nu$(OD)
SiOH	3745	(−100)[a]	—	—
(SiOH)*	3738	−162	2755	−125
$(AlOH)_1$	3660	−214	2700	−165
$(AlOH)_2$	3640	—	—	—
$Al^{VI}OH$	3715	—	—	—

[a] Literature value (see Ref. 16).

Hydrogen-bonding causes a shift in the stretching frequency of the involved hydroxyls; the extent of the shift is a measure of the OH acidity (16, 17). Because of the nearly total opaqueness in the range 3700–3620 cm^{-1}, it is difficult to observe shifts in the original spectra. These may, however, be appreciated in difference spectra such as those reported in Fig. 3, although absolute intensities in the above region have to be taken with care. Positive bands at 3236, 2859, 2389, and 2280 cm^{-1} are modes of the benzene molecule. Negative bands at 3738 and 3660 cm^{-1} are due to the OH species engaged in H-bonding, which correspond to positive bands at about 3578 and 3446 cm^{-1}; shifts are 162 and 214 cm^{-1}, respectively. The former band corresponds to (SiOH)*, the latter to $(AlOH)_1$; other hydroxyl species, e.g., $(AlOH)_2$, do not react. Further information on the H-bonding ability of the two types of hydroxyl is obtained after isotopic exchange.

Isotopic Exchange with Heavy Water and Benzene

A different measure of the propensity of hydroxyls to yield up their protons is deuteration. Again, the OH

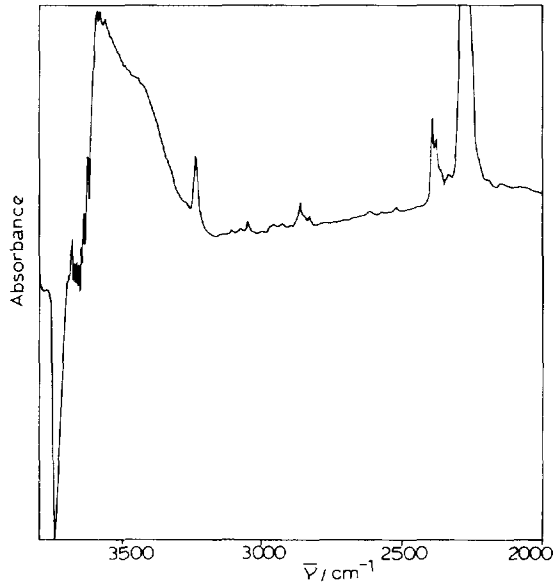

FIG. 3. IR difference spectrum illustrating the shifts in the hydroxyl stretching mode caused by adsorption on clay A outgassed at 770 K of C_6D_6 at 6 Torr pressure.

stretching region is difficult to study, while the corresponding OD region (2800–2500 cm^{-1}) is much more transparent. Moreover, the extinction coefficient of deuteroxyls is twice as great as that of hydroxyls. Figure 4 shows the room-temperature interaction of heavy water with clay A outgassed at 770 K. Exchange, monitored by absorption in the range 2800–2000 cm^{-1} and erosion in the 3200–3500 cm^{-1} region, is already substantial after 15 min. Removal of heavy water allows the identification of the hydroxyl species which have undergone exchange. After evacuation at 770 K, the OD band envelope narrows to a peak at 2699 cm^{-1} with a shoulder at 2758 cm^{-1}. This latter corresponds to the 3738 cm^{-1} band of (SiOH)*; the isotopic ratio is 1.356, in agreement with that found by Kazansky *et al.* for both SiOH and the bridged species Si(OH)Al in zeolites (18). This value allows us to relate the 2699 cm^{-1} peak to the 3660 cm^{-1} band in the OH region, i.e., to the species $(AlOH)_l$. It is most significant that the component at 3640 cm^{-1}, for which the OD equivalent would absorb at 2684 cm^{-1}, is not formed.

Deuteration with D_2O is extensive. Caution must be exercised in interpreting the results in Fig. 4, because water might be able to hydrolyze Si–O–Al bonds, giving rise to new OD groups. Indeed, we have evidence that ammonia does so (19). Support for the interpretation, however, comes from the use of the much milder deuterating agent C_6D_6 (Fig. 5), which does not exchange on clay A either at room temperature or after 1 h at 470 K. Deuteration occurs above 570 K; again, two peaks are observed at 2700 and 2755 cm^{-1}, after removal of the gas phase.

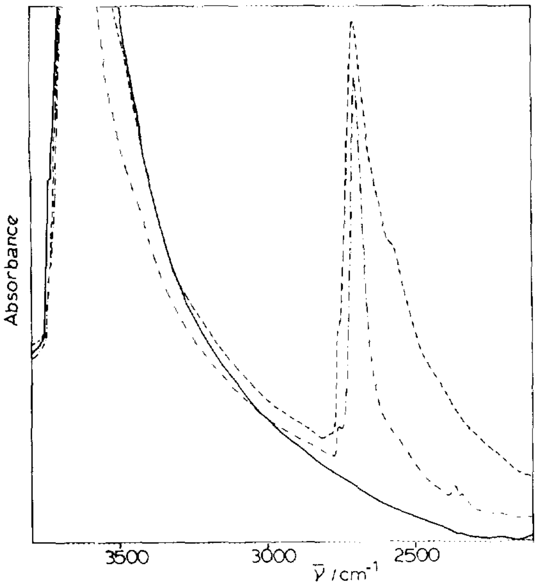

FIG. 4. IR spectra illustrating the deuteration of clay A outgassed at 770 K with D_2O. (—) starting sample; (---) after room-temperature contact with 10 Torr D_2O for 15 min and evacuation at 370 K; (-·-) evacuation at 770 K.

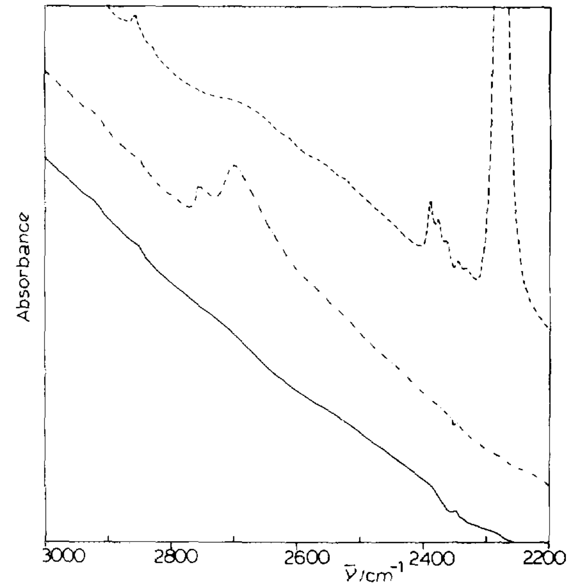

FIG. 5. IR spectra illustrating the deuteration of clay A outgassed at 770 K with C_6D_6. (—) starting sample; (---) after heating at 470 K under 6 Torr C_6D_6; (-·-) after heating at 570 K and successive evacuation.

Before evacuation, deuterobenzene interacts via hydrogen bonding with the few deuteroxyls which have been formed (difference spectrum in Fig. 6). Positive bands at ≈2630 and ≈2540 cm^{-1} are due to the OD species engaged in H-bonding, originally at 2700 and 2755 cm^{-1} (Table 1). (SiOD)* species shift by ≈125 cm^{-1}, which corresponds to ≈170 cm^{-1} in the O–H region, when the isotopic factor 1.356 is taken into account; $(AlOD)_l$ species shift by ≈165 cm^{-1}, which corresponds to ≈224 cm^{-1}. Such values are

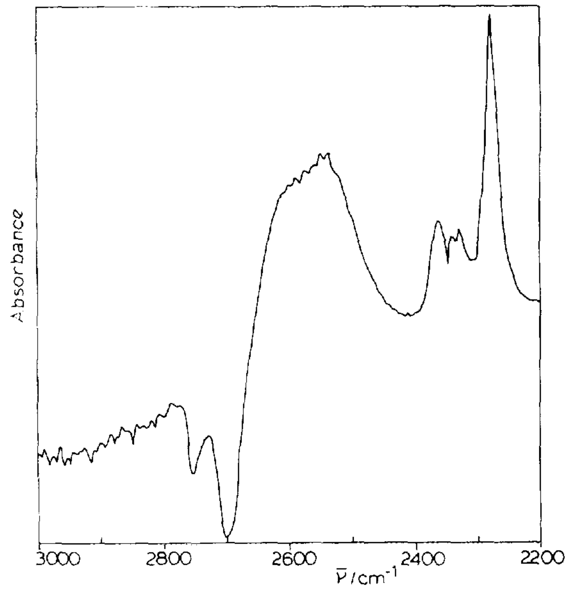

FIG. 6. IR difference spectrum illustrating the shifts in the deuteroxyl stretching mode caused by adsorption on clay A outgassed at 770 K of C_6D_6 at 6 Torr.

in excellent agreement with the shifts directly observed in the O–H region, reported in Table 1.

Pyridine Adsorption

Experiments were carried out on all three kinds of samples. As regards clay G, no pyridinium ions were formed, since the typical band manifold at 1639, 1621, 1493, and 1548 cm^{-1} was not observed on the sample outgassed at 670 K, in agreement with the observation (2, 3) that pyridinium ions are promoted by molecular water. Lewis sites were instead observed, stronger than Brønsted sites; the corresponding 8a mode of pyridine species adsorbed on Lewis acid sites is at 1612 cm^{-1}.

Adsorption of pyridine on clay A outgassed at 770 K is illustrated in Figs. 7–9. Figs. 7 and 8 describe reversible adsorption. Figure 7 reports the changes occurring in the ring-mode region of pyridine; Fig. 8 describes the changes occurring in the OH stretching region. Bands due to liquid-like pyridine are readily identified at 1582 (mode 8a), 1484 (mode 19a) and 1440 cm^{-1} (mode 19b). The pressure-dependent band at 1597 cm^{-1} is related to a labile species. Although it may also be due to weak Lewis sites, we ascribe it to the 8a mode of hydrogen-bonded pyridine, because it is very close to the corresponding mode of pyridine on silica (20). On the other hand, spectra in Fig. 8 show that the intensity of the band at 3738 cm^{-1} decreases strongly upon adsorption, and increases back with outgassing. The assignment of this band to the (SiOH)* species is therefore suggested. There is no evidence, however, that such hydroxyls, acidic enough to bind pyridine, may transfer the proton.

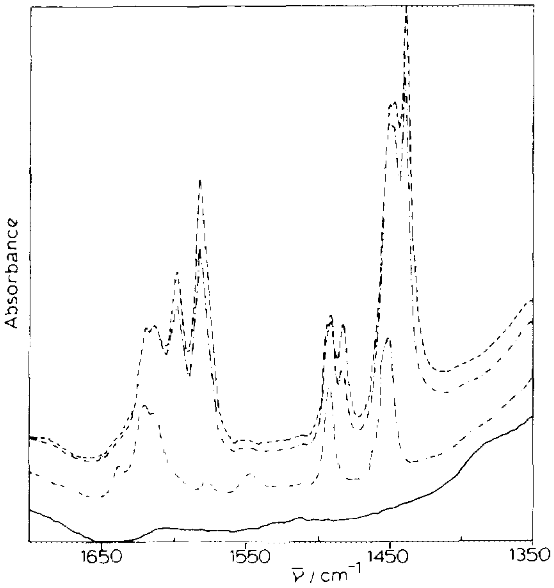

FIG. 7. IR spectra concerning reversible pyridine adsorption on clay A outgassed at 770 K. Pyridine ring-modes region. (—) starting sample; (---) with pyridine at 10 Torr; (-·-) evacuation at room temperature; (------) evacuation at 370 K.

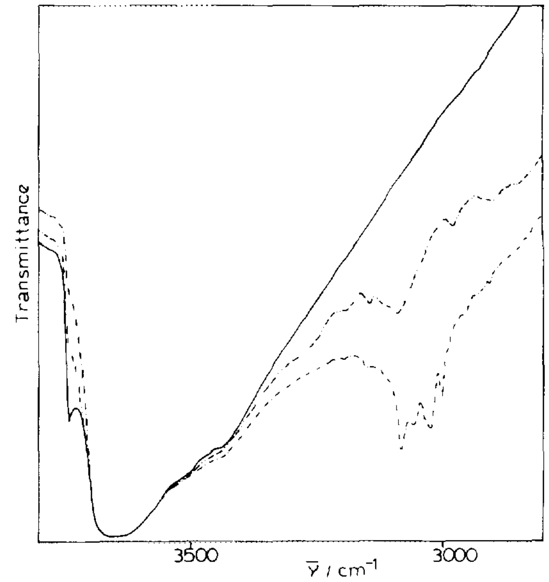

FIG. 8. IR spectra concerning reversible pyridine adsorption on clay A outgassed at 770 K. Hydroxyl stretching region. Curves as in Fig. 7.

Formation of pyridinium ions is, however, documented by the bands at 1639, 1621, 1493, and 1548 cm^{-1}; in the C–H stretching region, a doublet at 3250 and 3192 cm^{-1} in Fig. 8 is also due to this species. It is therefore straightforward to ascribe the formation of pyridinium species to the other acidic hydroxyl species, i.e., $(\mathrm{AlOH})_{\mathrm{I}}$.

Figure 9 illustrates the irreversible adsorption of pyridine and further changes induced by thermal treatments. Molecular pyridine bound to Lewis sites is responsible

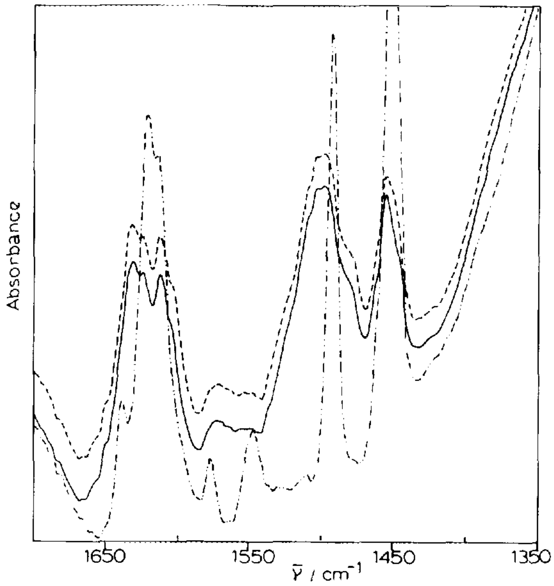

FIG. 9. IR spectra concerning irreversible pyridine adsorption on clay A outgassed at 770 K; continuation of the experiment in Fig. 7. (------) evacuation at 370 K; (—) evacuation at 570 K; (---) evacuation at 770 K.

for the bands at 1577, 1493, and 1452 cm^{-1}, and in particular for two components at 1621 and 1614 cm^{-1}, ascribable to the 8a mode of pyridine on two different Lewis sites.

After thermal treatment at 570 K *in vacuo*, new bands at 1635, 1503, 1483, and 1455 cm^{-1} are seen, growing at the expense of the pyridine species, whose 8a mode is at 1621 cm^{-1}. A further increase is caused by heating at 770 K. A similar process has been observed on transition aluminas (21) and ascribed to the reaction of a Lewis-coordinated pyridine molecule with a nearby hydroxyl to form α-pyridone and hydrogen (Scheme 1).

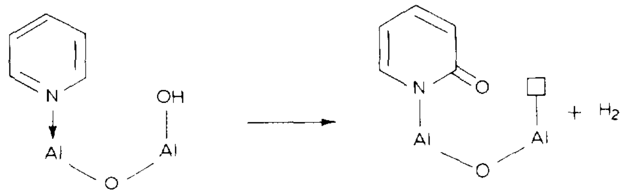

SCHEME 1

Adsorption of pyridine on clay A also has been studied after outgassing at 670 K only, instead of the standard treatment at 770 K described so far (figures are not reported). It is noteworthy that the relative overall intensity of the spectra decreases for an increase in pretreatment temperature; as a concomitant decrease in Lewis acidity is not expected, this is probably evidence that some collapse in the structure has taken place at 770 K. In the spectrum of pyridine irreversibly held on clay A treated at 670 K, the two peaks at 1621 and 1614 cm^{-1} are not resolved, and only one band is seen around 1620 cm^{-1}, although rather broad. Such a sample does not yield α-pyridone for the thermal treatments at 570 or 770 K.

DISCUSSION

Five different kinds of hydroxyl have been identified, absorbing at 3747, 3738, 3715, 3660, and 3640 cm^{-1}, respectively; evidence gathered is reported in Table 1. The peak at 3738 cm^{-1} is assigned to isolated silanols, designated by (SiOH)*, which are close in nature to (but do not coincide with) the well-known species which absorb at 3747 cm^{-1} on silica (14) and which are also present in the starting montmorillonite; the new species is produced by the pillaring process. The difference in stretching frequency, although small on an absolute scale, is, however, rather meaningful, and corresponds to a marked acidic character of (SiOH)*, shown by all types of acidity measurement adopted in the present work. Indeed, the new species undergoes isotopic exchange even with a mild agent like deuterated benzene and exchanges readily for Ce^{3+}. As to its tendency to bind benzene via H-bonding, it is worthy of note that the shift undergone by SiOH in zeolites upon coordination of benzene is only 100 cm^{-1} (16), whereas that measured here for (SiOH)* is some 160 cm^{-1}; this is clear proof of a larger acidic character. The acidity of such hydroxyls is, however, lower than that of the (AlOH)$_1$ species absorbing at 3660 cm^{-1}, which undergoes a shift of 224 cm^{-1}. (SiOH)* hydroxyls are probably not acidic enough to transfer their protons to pyridine, and only H-bonding occurs, giving rise to the molecular species whose 8a mode is at 1597 cm^{-1}. A structure accounting for all the above observations is shown in Scheme 2; it arises by sealing the pillar and the clay sheet together. The hydroxyl under discussion appears as basically a silanol species which is formed on the clay sheet by tetrahedra inversion or a similar mechanism, perturbed by an adjacent Al ion.

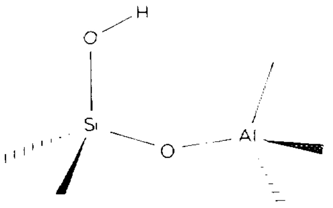

SCHEME 2

The shoulder at 3715 cm^{-1} is probably related to hydroxyls octahedrally coordinated on aluminum as bands in such a position are found, e.g., on α-alumina samples (14). The bands at 3660 and 3640 cm^{-1} are also probably both due to hydroxyls sitting on aluminum ions, and have accordingly been designated so far by (AlOH)$_1$ and (AlOH)$_2$. The acidic behavior of the two hydroxyls is, however, drastically different. The species absorbing at 3660 cm^{-1} is the most acidic hydroxyl in the systems studied, whereas the species absorbing at 3640 cm^{-1} is not acidic at all. As to their location, the choice is between Al sites in the octahedral layers or in pillars. The ready accessibility to benzene molecules, both for H-bonding and for isotopic exchange, suggests pillars as the sites where (AlOH)$_1$ species are located and the octahedral layers for the (AlOH)$_2$ sites.

In agreement with such an assignment for (AlOH)$_2$, we may note that in transition aluminas (14), hydroxyls which are nonacidic are found absorbing at 3660–40 cm^{-1}. As to (AlOH)$_1$, one may recall that in dealuminated HY zeolites, strongly acidic hydroxyls are present at around 3645 cm^{-1} on extraframework aluminum ions located in large cavities (14). A band at 3670–60 cm^{-1} is present in HZSM 5 zeolites and mordenite, whose fairly acidic nature has been established by CO adsorption (17, 22). The structure shown in Scheme 3, involving extraframework Al, has been recently proposed (22).

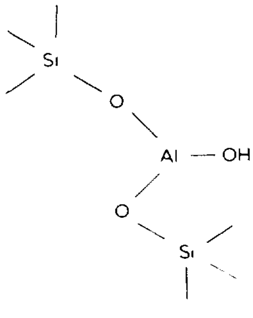

SCHEME 3

On this basis, a possible structure for $(\mathrm{AlOH})_l$ accounting for the available evidence is that shown in Scheme 4. Also, such species may be thought of as arising by sealing together Al pillars and siliceous clay sheets and may be understood as the counterpart of the structure proposed for (SiOH)* species.

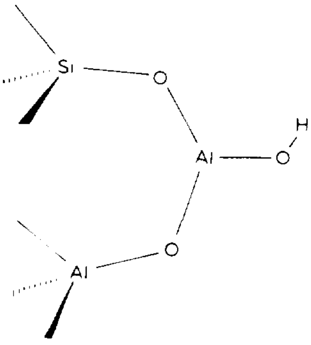

SCHEME 4

The hydroxyl under examination, although markedly acidic, is, however, less so than the bridged hydroxyl in zeolites, whose stretching frequency is displaced by some 300 cm^{-1} by interaction with benzene (16).

It is appropriate to note that no bridged hydroxyl Si(Al)OH is observed; this species absorbs at 3610 cm^{-1} on zeolites. Substitution of Si for Al does not take place in the tetrahedral layer of montmorillonites, so that such species are not present in the starting material; furthermore, the process of sealing the clay sheet and the pillar together does not produce bridging OH species.

In conclusion, the Brønsted acidic behavior in Al-pillared montmorillonite (at least that observable after thermal treatment at 770 K) seems to arise from the synergy of the siliceous clay sheet and the pillar, in agreement on the one hand with what has been already reported (9, 10), and in contrast, on the other hand, with the view that locates the Brønsted sites only in the clay sheet (11).

As to Lewis sites, pyridine adsorption shows that at least two sites are present, clearly seen after thermal pretreatment at 770 K, both ascribable to Al centers. This is not surprising, as transition aluminas show two Lewis species with values of the 8a mode close to the present ones (14). Because clay G only shows the site characterized by a lower 8a frequency, it is tempting to ascribe the 1614 cm^{-1} species to Al sites in the tetrahedral layer (we assume that pyridine is not likely to reach the octahedral layer), and the 1621 cm^{-1} species to Al sites on pillars, absent on clay G. The transformation of pyridine into α-pyridone is likely to take place on this latter type of site. It has to be noted that, according to Scheme 1, pyridone formation requires the intervention of a nearby *basic* hydroxyl, performing a nucleophilic attack in the α-position of pyridine; the presence of nonacidic hydroxyls has indeed been documented in the present paper. The availability of such hydroxyls, e.g., in the octahedral layer, may account for the lower temperature of transformation with the present system than that observed for transition aluminas.

REFERENCES

1. Figueras, F., *Catal. Rev.* **30,** 457 (1988).
2. Wright, A. C., Granquist, W. T., and Kennedy, J. V., *J. Catal.* **25,** 65 (1972).
3. Mortland, M. M., and Raman, K. V., *Clays Clay Miner.* **16,** 398 (1968).
4. Mortland, M. M., Fripiat, J. J., Chaussidon, J., and Uytterhoeven, J., *J. Phys. Chem.* **67,** 248 (1963).
5. Zhougui, L., and Guida, S., *in* "Zeolites" (B. Držaj, S. Hočevar, and S. Pejovnik, Eds.), p. 493. Elsevier, Amsterdam, 1985.
6. Plee, D., Schutz, A., Poncelet, G., and Fripiat, J. J., *in* "Catalysis by Acids and Bases" (B. Imelik, C. Naccache, G. Coudurier, Y. Ben Taarit, and J. C. Védrine, Eds.), p. 343. Elsevier, Amsterdam, 1985.
7. Tichit, D., Fajula, F., Figueras, F., Guegen, C., and Bousquet, J., *in* "Am. Chem. Soc. Symposium on FCC, New Orleans, 1987," p. 647.
8. Shabtai, J., Massoth, F. E., Tokarz, M., Tsai, G. M., and McCauley, J., "Proceedings, 8th International Congress on Catalysis, Berlin, 1984," Vol. 4, p. 735. Dechema, Frankfurt-am-Main, 1984.
9. Occelli, M. L., and Tindwa, R. M., *Clay Miner.* **31,** 22 (1983).
10. Occelli, M. L., and Lester, J. E., *Ind. Eng. Chem. Prod. Res. Dev.* **24,** 27 (1985).
11. Ming-Yuan, H., Zhonghui, L., and Enze, M., *Catal. Today* **2,** 321 (1988).
12. Tichit, D., Fajula, F., Figueras, F., Bousquet, J., and Guegen, C., *in* "Catalysis by Acids and Bases" (B. Imelik, C. Naccache, G. Coudurier, Y. Ben Taarit, and J. C. Védrine, Eds.), p. 351. Elsevier, Amsterdam, 1985.
13. Tichit, D., Ph.D. Thesis, Université de Montpellier, 1986.
14. Zecchina, A., Coluccia, S., and Morterra, C., *Appl. Spectrosc. Rev.* **21,** 259 (1985).
15. Plee, D., Borg, F., Gatineau, L., and Fripiat, J. J., *J. Am. Chem. Soc.* **107,** 2362 (1985).
16. Kustov, L. M., Kazansky, V. B., Beran, S., Kubelkova, L., and Jírů, P., *J. Phys. Chem.* **91,** 5247 (1987).
17. Garrone, E., Chiappetta, R., Spoto, G., Ugliengo, P., Zecchina, A., and Fajula, F., "Proceedings, 9th International Zeolite Conference, Montreal, 1992," Vol. 2, p. 267. Butterworth-Heinemann, Boston, 1993.

18. Kazansky, V. B., Gritscov, A. M., Andreev, V. M., and Zhidomirov, G. M., *J. Mol. Catal.* **72,** 149 (1989).
19. Garrone, E., and Bodoardo, S., unpublished.
20. Severdia, A. G., Morterra, C., and Low, M. J. D., *J. Colloid Interface Sci.* **99,** 208 (1984).
21. Knözinger, H., Krietenbrink, H., Muller, H. D., and Schultz, W., "Proceedings, 6th International Congress on Catalysis, London, 1976" (G. C., Bond, P. B. Wells, and F. C. Thompkins, Eds.), Vol. 1, p. 183. The Chemical Society, London, 1977.
22. Zecchina, A., Bordiga, S., Spoto, G., Scarano, D., Petrini, G., Leofanti, G., Padovan, M., and Otero Areán, C., *J. Chem. Soc. Faraday Trans.* **88,** 2959 (1992).